

Precision improvement and reduction of blind zones in ultrasonic transducers Golay complementary sequences

Amélioration de la précision et réduction des zones
masquées de capteurs à ultrasons grâce à l'utilisation
de séquences complémentaires de Golay

**Alvaro Hernández¹, Jesus Ureña¹, Manuel Mazo¹,
José A. Jiménez¹, Juan Jesus García¹, Fernando Álvarez²,
Jean-Pierre Dérutin³ et Jocelyn Sérot³**

¹Electronics Dept. Polytechnic School. University of Alcalá. E28806 Alcalá de Henares Madrid (Spain),
alvaro@depeca.uah.es

²Dept. of Electronics and Electromechanics Engineering. University of Extremadura. E.P. Campus Universitario, Cáceres (Spain)

³LASMEA Laboratory. Université Blaise Pascal. F63177 Aubière (France)

Manuscrit reçu le 15 janvier 2004



Abstract and key words

Sensorial systems based on ultrasonic transducers present some constraints, which reduce their performances. Typical problems are low precision in measurements, and the existence of a blind zone in front of transducers, where reflectors can not be detected if transducers are used as emitters and receivers. In order to improve the precision achieved by these transducers, binary sequences are often used to code the emission, so afterwards, distances can be determined using correlation techniques. The usage of Golay complementary sequences allows to increase remarkably the precision obtained by an isolated ultrasonic transducer. Also, it permits to eliminate the mentioned blind zone, thanks to their auto-correlation characteristics. These two features are very interesting in order to use ultrasonic transducers in more complex sensorial associations.

Ultrasonic sensorial systems, Golay complementary sequences, precision improvement, reduction of blind zones.

Résumé et mots clés

Les systèmes sensoriels basés sur les capteurs à ultrasons présentent certaines contraintes qui ont tendance à réduire leur performance. Parmi les problèmes typiques, nous pouvons citer la faible précision des mesures et l'existence à l'avant des capteurs de zones masquées, zones où les réflecteurs ne peuvent pas être détectés si les capteurs sont utilisés comme émetteurs et récepteurs. Dans le but d'améliorer la précision des mesures réalisées par ces capteurs, les émissions sont le plus souvent codées par des séquences binaires. Les distances peuvent être alors déterminées en faisant appel à des techniques de corrélation.

Dans ce cadre, ce travail présente les résultats obtenus lors de l'utilisation de séquences complémentaires de Golay, lesquelles permettent d'augmenter de manière significative la précision obtenue à partir d'un capteur à ultrasons isolé.

Elles permettent également d'éliminer les zones masquées précédemment citées grâce à leurs caractéristiques d'auto-corrélation. Ces deux fonctions seront très intéressantes dans l'optique d'une utilisation de capteurs à ultrasons dans le cadre d'associations sensorielles plus complexes.

Systèmes sensoriels à ultrasons, séquences complémentaires de Golay, amélioration de la précision, réduction des zones masquées.

Acknowledgements

This work has been possible thanks to the Ministerio de Ciencia y Tecnología from Spain: PARMEI project (ref. DPI2003-08715-C02-01); to the Comunidad de Madrid from Spain: ENIGMA project (ref. 07T/0051/2003); and to the University of Alcalá: ISUAP project (ref. PI2004/033).

1. Introduction

Sonar systems have been installed on mobile robots, trying to take advantage of their simplicity and their low cost. A typical technique to process ultrasonic signals is based on the measurement of times-of-flight (TOF). This type of processing has been always characterized by some constraints, either in isolated transducer or in sensor arrays:

- Precision in measured distances is low. This can be enough for some simple applications, but not to process measurements from different transducers in more sophisticated systems. In these systems it is possible to determine the reception angle (lateral resolution), or to perform a reflector classification (*i.e.*, walls, edges, corners), mapping, etc, if TOFs are precise enough. There are different works focused on these tasks [Barshan] [Kleeman 1] [Kleeman 2].
- In most proposed sonar systems [Elfes] [Jörg], the use of a transducer as emitter/receiver implies the appearance of a blind area in the surroundings of the transducer. Basically, the coupling of the emission into the reception circuit avoids that reflectors can be detected when they are very close to transducers. So an obstacle will not be detected, if it is located at a smaller distance than the one traveled by the pulse-wave during the emission interval [Borestein] [Peremans] [Ureña 1] [Polaroid] [Kleeman 2].

In this work, a novel ultrasonic processing system is proposed, in order to mitigate problems related to the previous items. Section 2 explains the sensorial structure used. Section 3 describes the proposed processing algorithms. Section 4 deals with the precision achieved in the determination of TOFs. How it is possible to eliminate the blind area of an ultrasonic transducer is shown in section 5. And, finally, some conclusions are discussed in section 6.

2. Sensorial structure proposed

The sensor configuration used can be seen in Figure 1. It is the geometrical association of four transducers. Every two transducers constitutes a "vector sensor", able to measure distances and reception angles [Ureña 1]. These transducers are very close to each other to minimize correspondence problems and to confirm the reception of echoes from the same reflector by both transducers [Peremans] [Ureña 1] [Kleeman 1]. The two transducers *E/R1* and *E/R4*, placed at both ends, work as emitter/receivers, whereas transducers *R2* and *R3* are only receivers. In Figure 1, *P* is a possible reflector, detected by the four transducers (r_1 , r_2 , r_3 and r_4). On the other hand, Figure 2 shows a view of the structure developed.

This sensor configuration type and its use have been described in [Kleeman 1] [Ureña 2] [Hernández 1] in order to classify different reflector types or to build maps of the environment [Hernández 2]. If it is desirable to improve the capability of these sensors, it is important to achieve the following features:

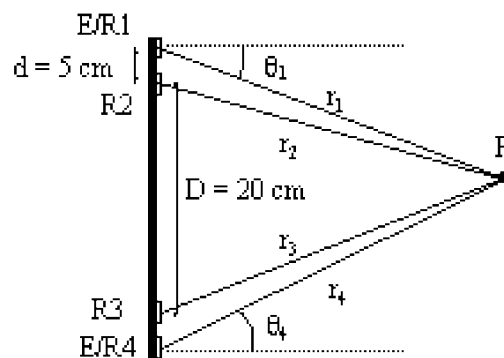


Figure 1. Sensor composed of four ultrasonic transducers.

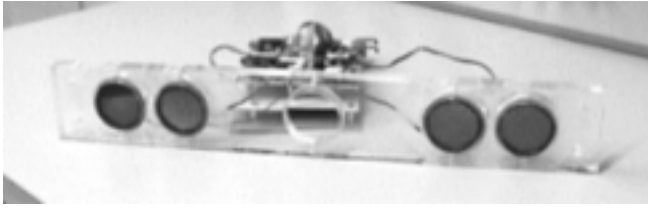


Figure 2. General view of the sensorial structure developed.

- Precision is basic, since later reflector classifications or mapping tasks are usually based on geometrical considerations. In this way, it is desirable to develop an ultrasonic sensorial systems where a high precision is achieved, and a suitable immunity to noise is provided.
- Finally, there are two transducers, $E/R1$ and $E/R4$, working as emitter/receivers, so initially they present a blind zone where it is not possible to detect any reflector. The dimension of this area depends on the length of the ultrasonic emission, so a careful selection can improve this constraint considerably.

Also, it is usually desirable to have simultaneous reception of the reflected signal by all the transducers ($E/R1$, $R2$, $R3$ and $E/R4$). In this way, four TOF measurements can be combined in high-level algorithms from just one emission. Furthermore, the probability of obstacle detection is increased and problems related to specular reflections are reduced. On the other hand, echo discrimination can distinguish which transducer emitted the signal ($E/R1$ and $E/R4$ in Figure 1), even if the emissions from both transducers are simultaneous. This is possible thanks to the ultrasonic pulse codification used in each emitter. In this way, it is possible to carry out simultaneous emissions without crosstalk interferences, reducing the scanning time and obtaining several echoes for a reflector from different emission sources. Although multi-mode techniques (simultaneous emission and reception) are not developed in this work, they are also supported by the algorithms here presented [Hernández 1].

Next sections describe a novel algorithm for the determination of TOFs, meeting the requirements mentioned before (high precision and blind zone reduction). Methods and results will be commented only for one transducer of the sensor array, assuming the same conclusions for the rest working in the mentioned sensorial structure.

3. Measurements of TOFs

Different proposals have been carried out to determine TOFs; some of them have been led to the code of binary sequences in the emission of transducers [Hovanessian] [Peremans] [Audenaert]. These sequences have a high auto-correlation function, so the determination of TOFs becomes a more immune processing to the noise influence.

There are numerous binary sequences, that can be used in this application area. Among them, the 13-bit Barker code is included [Audenaert] [Ureña 1], because of its high auto-correlation, but with the drawback of not having orthogonal sequences with the same length; also its length is constrained at only 13 bits. Pseudo-random sequences have been also used [Shoval] because they meet conditions of high auto-correlation, and there are several orthogonal sequences; but on the contrary, their features imply their periodical emission, so transducers can not be used as emitters and receivers in the same system.

The analysis here presented has been focused on a pair of Golay complementary sequences [Golay] [Tseng]. Usually Golay codes have been used to improve quality and to enhance SNR ratios in ultrasonic imaging for biomedical applications [O'Donovan] [Yoo] [Kim]. Nevertheless, the feasibility of these codes applied to ultrasounds in mobile robots have been also shown in some previous works. In [Hayward] a first proposal is done, developing a fast digital hardware correlator for low-power ultrasonic applications by means of Golay sequences. Also, they have been used for obstacle detection in mobile robots [Lee] [Diaz].

A Golay pair is composed of two sequences, $A[n]$ and $B[n]$, where the addition of both independent auto-correlation functions provides an ideal signal according to (1).

$$C_{AA}[n] + C_{BB}[n] = \begin{cases} 2N & n = 0 \\ 0 & n \neq 0 \end{cases} \quad (1)$$

Where $A[n]$ and $B[n]$ are sequences with values in $\{-1, +1\}$; N is the number of bits, or the length of sequences; and $C_{AA}[n]$ and $C_{BB}[n]$ are the auto-correlation functions of both sequences, $A[n]$ and $B[n]$ respectively. Figure 3 shows the result of this process for a 32-bit Golay complementary sequence pair.

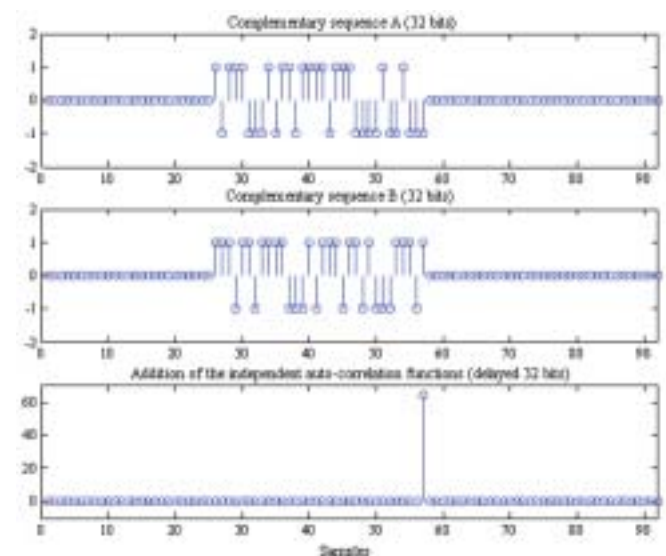


Figure 3. Example of auto-correlation for 32-bit Golay sequences.

It is possible to find two different and orthogonal Golay complementary sequence pairs, what allows the development of multi-mode techniques in sonar systems [Hernandez 1] with non-periodical correlations.

3.1. Ultrasonic emission

As has been mentioned, next explanations are focused on only one transducer, which is integrated in a sensorial array composed of four transducers. The algorithms, here proposed for a transducer, are also suitable for the rest, being only necessary to assign different orthogonal Golay pairs to every emitter in the sensorial structure (avoidance of crosstalk interferences) [Hernández 1]. In order to achieve more generalization in the definition of the algorithms, one generic ultrasonic transducer is assumed, denoted by the subscript i .

The used ultrasonic transducer has the maximum frequency response at 50kHz [Polaroid], so a modulation of the Golay sequence pair with a carrier of that value has been carried out. A digital variant of a QPSK modulation has been used [Díaz], where sequences A and B , both from the same pair of complementary sequences, have been associated to components I and Q in the modulation, respectively. In [Lee] a different method is proposed, based on the consecutive emission of complementary sequences A and B . However, this solution has been discarded, as it requires a static environment, with non-moving sensors or reflectors. In this way, QPSK modulation allows both complementary sequences to be emitted simultaneously, so motion can be supported by the final system.

Equation (2) describes this modulation process, to obtain the signal $e_i[n]$ emitted by transducer i . The N -bit Golay pair is obtained according to the Efficient Golay Generator (EGG) scheme proposed by [Budisin] [Popovic] using a seed \mathbf{W} with s bits, where $2^s = N$. The Golay pairs generated by means of the EGG structure have some particular features, which, afterwards, can be used to simplify the correlation process.

$$\begin{aligned}
 e_i[n] &= A_i[n] * S_I[n] + B_i[n] * S_Q[n] = \\
 &= \sum_{k=0}^{N \cdot M \cdot m - 1} A_i \left[\frac{k}{M \cdot m} \right] S[n - k] \\
 &\quad + \sum_{k=0}^{N \cdot M \cdot m - 1} B_i \left[\frac{k}{M \cdot m} \right] S \left[\left(n - \frac{M}{4} \right) - k \right] \quad (2)
 \end{aligned}$$

Where M is the number of samples per period of the symbol $S[n]$ (related to the sampling frequency f_s of the received signal); m is the number of periods per symbol; and N is the number of bits or the sequence length. The signals $A_i[n]$ and $B_i[n]$ constitute the Golay pair assigned to the emitter i . On the other hand, the signals $S_I[n]$ and $S_Q[n]$ are the carriers of components I and Q, obtained from the symbol $S[n]$ with the corresponding delay. As has been already mentioned, the symbol allows the emission to be focused at a 50kHz frequency; so, a sampling frequency f_s of 400kHz has been fixed, with enough

oversampling to have suitable results. Because of that, $M = 8$ and $m = 2$ have been configured. The selected value for M allows to recover correctly the emitted signal. Whereas, the parameter m is related to the energy used for every emission and the bandwidth. The symbol $S[n]$ can be represented as a sequence, according to (3).

$$\begin{aligned}
 S[n] &= [1100 - 1 - 1001100 - 1 - 100] \\
 S_I[n] &= [1100 - 1 - 1001100 - 1 - 100] \\
 S_Q[n] &= [00 - 1 - 1001100 - 1 - 10011] \\
 S_Q[n] &= S_I[n - 2] \quad (3)
 \end{aligned}$$

3.2. Correlating Golay complementary sequences

Once emitted the signal $e_i[n]$ by the corresponding transducer i , it travels through the environment, returning back to transducers after reflecting against possible obstacles. In order to determine the ultrasonic TOFs accurately, it is necessary to carry out a continuous searching of possible echoes in the signal captured by a transducer. For that reason, the first step in the reception process consists of the demodulation of the received signal in order to extract components $I_i[n]$ and $Q_i[n]$ from the signal $r_i[n]$ received by transducer i , according to (4). The signal $S[n]$ is the modulation symbol again.

$$\begin{aligned}
 I_i[n] &= C_{rS_I}[n] = r_i[n] * S_I[n] \\
 &= \sum_{k=0}^{N \cdot M \cdot m - 1} r_i[k + n] S[k] \\
 Q_i[n] &= C_{rS_Q}[n] = r_i[n] * S_Q[n] \\
 &= \sum_{k=0}^{N \cdot M \cdot m - 1} r_i[k + n] S \left[k - \frac{M}{4} \right] \quad (4)
 \end{aligned}$$

Analyzing the symbols for every component, $S_I[n]$ and $S_Q[n]$, shown in (3), it can be observed that the two necessary correlations to obtain components $I_i[n]$ and $Q_i[n]$ are redundant, as both symbols are equal, apart from a displacement of two samples (actually $M/4$ samples). For that reason, the demodulation process can be reduced to a single correlation operation that allows to obtain the component $Q_i[n]$, keeping in mind that $I_i[n]$ can be obtained from the previous one by means of a $M/4$ -sample delay. It is important to remark that this simplification is only possible thanks to the features of the used symbol $S[n]$: it has $M/4$ null samples at the end of every period -see (3)-.

Once obtained the signals $I_i[n]$ and $Q_i[n]$, the following step is to carry out the searching of Golay sequences, each one of them in its corresponding component. This operation could be carried out by means of a classical correlation, what would allow to detect the emitted pair. But, the method proposed in [Budisin] and [Popovic] can be used to improve performances and resource requirements. It is an optimized method, called Efficient Golay Correlator (EGC). This model allows to simplify the

detection process, whenever Golay sequences with a length N power of 2 are used ($N = 2^s$, where s is the number of bits of the sequence seed \mathbf{W} , such that $\mathbf{W} = [w_0, w_1, \dots, w_{s-1}]$). The block diagram in Figure 4 shows this algorithm.

Where D_s means a delay module $D_s = 2^{P_s}$; P_s is any permutation of the numbers $\{0, 1, \dots, s - 1\}$, represented as $\{w_0, w_1, \dots, w_{s-1}\}$; $C_{rA}[n]$ and $C_{rB}[n]$ are the results of the correlation between the input signal $r[n]$ and the pair of Golay sequences A and B , generated using the seed \mathbf{W} . These results will be added and analysed to detect the received echoes.

The scheme can be adapted easily to the proposed algorithms; if a demodulation component, $I_i[n]$ or $Q_i[n]$, is applied to the EGC input, the correlation results between this component and the sequences $A_i[n]$ and $B_i[n]$ are obtained at the output.

Considering this idea, this diagram has to be adapted to the specifications of the current proposal. It should be kept in mind that only the in-quadrature component $Q_i[n]$ is calculated. Now, this component becomes the input of the EGC correlator, in such a way that, at the output, the result of the correlation of the component $Q_i[n]$ by the sequence $A_i[n]$ is obtained at the top branch, $S_{Q_i A_i}[n]$, and by the sequence $B_i[n]$ at the bottom one, $S_{Q_i B_i}[n]$. The sequence $A_i[n]$ should really be correlated by the component $I_i[n]$. The best solution consists of introducing a delay at the output of the top branch of the EGC. The result of the top branch must be stored for $M/4$ cycles in order not to be used until its homologous from the bottom branch is available. In this way, the signal $S_{I_i A_i}[n]$ is obtained, and added to $S_{Q_i B_i}[n]$, providing the final signal of the process $s_i[n]$. Figure 5 shows this adaptation using the general EGC scheme, where it can be observed also that delays D appear multiplied by a factor $M \cdot m$ ($M = 8, m = 2$). This factor is fixed by the decimation and by the number of periods per symbol $S[n]$ ($m = 2$). The decimation is necessary in the signal after the acquisition pro-

cess at a frequency $f_s = 400$ kHz, higher than the emitting one (50 kHz) ($M = 8$).

3.3. Local maximum detector

The purpose of this stage is the determination of the local maximum values in the processed signal $s_i[n]$, so they can be validated as echoes. The simplest method is based on the definition of a static threshold U_e , so all the samples that overcome this level become possible candidates. These candidates will be validated definitively as echoes in those cases where there is not another greater candidate around them. Using an analysis window, with a width of $2L$, the possibility of validating the secondary lobes as echoes is eliminated, as they will be discarded in presence of the main lobe. This procedure is described mathematically in (5).

$$\begin{aligned} &\forall m \in \{-L, -L + 1, \dots, -1, 1, 2, \dots, L - 1, L\} \\ &\text{if } s_i[n] > s_i[n + m] \text{ and } s_i[n] > U_e \\ & p_i[n] = 1 \\ & \text{else} \\ & p_i[n] = 0 \\ & \text{end if;} \end{aligned} \tag{5}$$

Where U_e is the fixed static threshold; L is the analysis window, which is usually determined to eliminate the secondary lobes produced by the non-coherent demodulation; and $p_i[n]$ is the validation signal of echoes from the emission in transducer i (this signal will have values in $\{0, 1\}$, being '1' the value for a validated echo). The value selected for U_e depends on the length N , so it is adapted experimentally to the maximum value provided by the correlation process. Concerning the parameter L , a

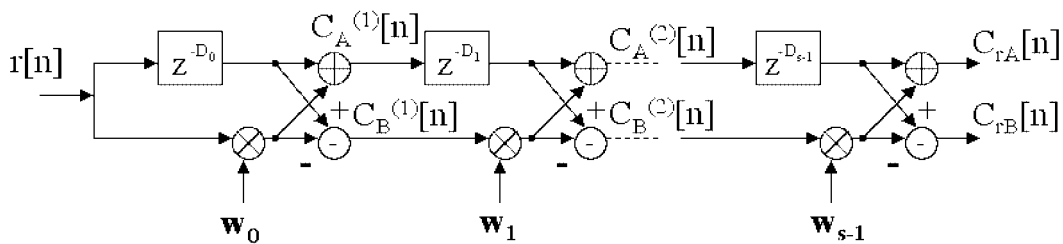


Figure 4. Block diagram of the Efficient Golay Correlator (EGC).

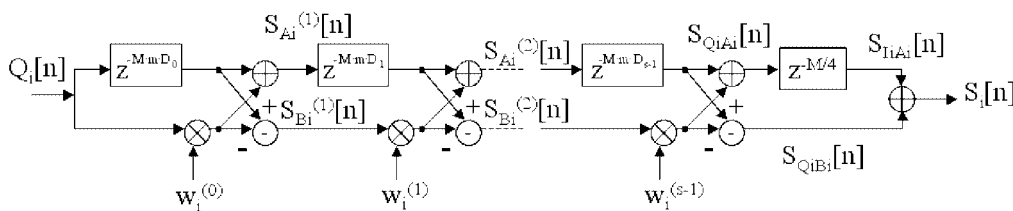


Figure 5. Modified block diagram of the Efficient Golay Correlator (EGC).

value of 16 samples has been configured, taking into account that $M = 8$ and $m = 2$.

3.4. General scheme of processing

A general block diagram about processing for a generic transducer i can be developed. This diagram, shown in Figure 6, depicts the different processing stages mentioned before, necessary in an emitter/receiver.

The used ultrasonic transducer is a Polaroid electrostatic device, together with a 6500 series module. This module has been modified to allow the input of any external signal $e_i[n]$ to emit.

4. Precision in TOF measurements

From a theoretical point of view, the minimum resolution in the determination of a measurement is provided by the sampling period T_s of the acquisition system. So, the signal $r_i[n]$ received by a transducer i is acquired at a frequency of 400 kHz, what implies a new sample $r_i[n]$ is available every $2.5 \mu s$. Supposing an ultrasonic propagation speed around $c = 340 \text{ m/s} = 0.34 \text{ mm}/\mu s$, the distance traveled by the wave during two successive samples is 0.85mm. This implies a maximum resolution of 0.425mm in the determination of the distance between a transducer i and the detected reflector (supposing that the ultrasonic wave flies through the environment and it returns back to the transducer).

From an experimental point of view, a statistical study has been carried out, placing an edge reflector (whose diameter is $\phi = 3,5 \text{ cm}$) at a distance d on the axial axis of the transducer i (see Figure 7). Two hundred measurements have been performed for every analysed distance d , calculating the averaged value for the obtained results, as well as the standard deviation σ_i . These parameters are shown in Table 1, for 32-bit Golay sequences,

whereas in Table 2 and Table 3 those same data are compiled for Golay sequences with lengths N of 64 and 128 bits.

The differences existing between the averaged values obtained in the measurements and the real distances d are always in the range of millimetres, likely due to errors in the positioning system used for such tests. On the other hand, the percentage of correct measurements makes reference to the amount of emissions that did not provide an echo, so the system did not obtain a valid TOF. This value usually depends on several external environmental parameters, as turbulences, air flows, ..., which have a direct influence on the ultrasonic performance. It can be

Table 1. Values obtained in the TOF determination at the mentioned distances for $N = 32$ bits, performing 200 measurements per distance.

$N = 32$ bits	Average value (cm)	σ_i (mm)	Correct measurements (%)
$d = 60 \text{ cm}$	60.65 cm	0.0946 mm	100%
$d = 100 \text{ cm}$	100.10 cm	0.1163 mm	98%
$d = 200 \text{ cm}$	200.18 cm	0.6923 mm	97%
$d = 300 \text{ cm}$	300.53 cm	1.0016 mm	100%

Table 2. Values obtained in the TOF determination at the mentioned distances for $N = 64$ bits, performing 200 measurements per distance.

$N = 64$ bits	Average value (cm)	σ_i (mm)	Correct measurements (%)
$d = 60 \text{ cm}$	60.05 cm	0.0611 mm	99%
$d = 100 \text{ cm}$	100.00 cm	0.1036 mm	99%
$d = 200 \text{ cm}$	200.25 cm	0.2361 mm	100%
$d = 300 \text{ cm}$	300.20 cm	0.8712 mm	97%

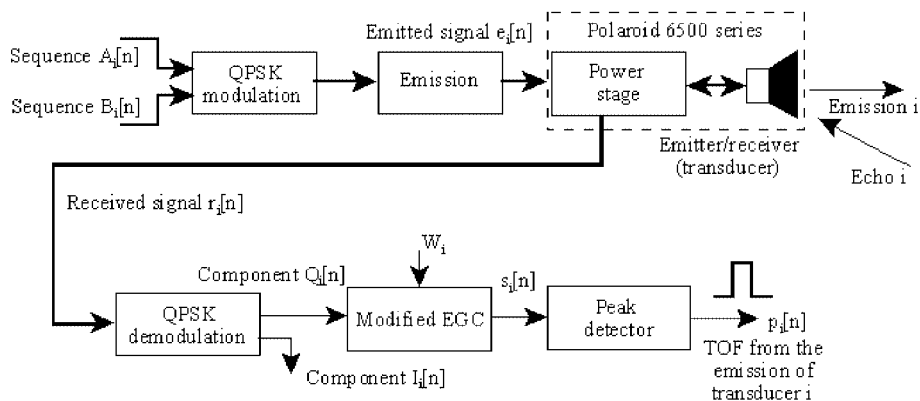


Figure 6. Block diagram of the processing associated to a transducer i .

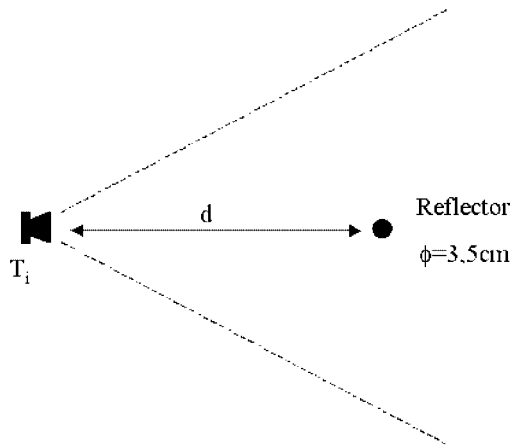


Figure 7. Experimental tests in order to compute the precision obtained in the TOF determination.

Table 3. Values obtained in the TOF determination at the mentioned distances for $N = 128$ bits, performing 200 measurements per distance.

$N = 128$ bits	Average value (cm)	σ_i (mm)	Correct measurements (%)
$d = 60$ cm	60.05 cm	0.0432 mm	100%
$d = 100$ cm	100.00 cm	0.1036 mm	99%
$d = 200$ cm	200.25 cm	0.1079 mm	100%
$d = 300$ cm	299.97 cm	0.4670 mm	98%
$d = 400$ cm	400.39 cm	0.8540 mm	96%
$d = 500$ cm	500.18 cm	0.9563 mm	97%
$d = 600$ cm	600.74 cm	1.5120 mm	96%

observed as, in most analysed cases, 100% of emissions were processed correctly; and in those cases where errors took place, these never were higher than 3% of emissions.

The parameter of the standard deviation σ_i is more interesting. The value is a repetition index about the measurement, and therefore an indication about its precision. Obviously, when this deviation is lower than 0.45 mm, the theoretical boundary from the acquisition system will be more restrictive. When the distance d increases, the system benefits begin to be degraded, so the standard deviation of measurements increases overcoming the theoretical constraint of 0.45 mm. So far, the precision in measurements begins to be limited by other external factors. This fact justifies the use of longer sequences when distance increases, in order to keep approximately constant some conditions of precision and deviation σ_i , or at least below the theoretical value, at any point in the environment.

Carrying out a comparison with other previous systems, the standard deviations σ_i here obtained are lower than those from most works in the area [Sabatini] [Peremans] [Papageorgiou] [Ureña 1]. Only, more recent works as [Kleeman 2] have achieved even better values for σ_i (around 0.2 mm for distances of 300 cm), although with a considerable increase in the computational load since they are based on the searching of reception patterns. It is also necessary to mention that the system here described could be improved notably increasing the sampling frequency f_s , what would provide a higher precision with a reduced increment of the computational requirements. It should be also considered that the reflector used in these measurements is a small pole with a specular surface; results would have been better if planes, or other types of obstacles, had been used.

Figure 8 shows an example about a real scenario where an edge reflector has been placed on the axial axis of the transducer at a distance d of 153 cm.

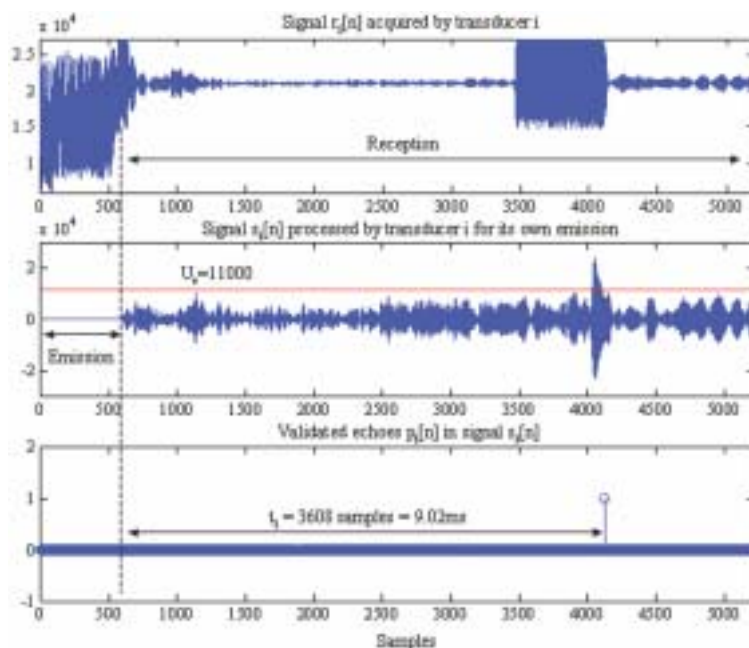


Figure 8. Processing example of an environment with an edge reflector at 153 cm.

5. Reduction of the blind zone

As has been mentioned, most proposed sonar systems are not able to detect reflectors, that are next to them [Elfes] [Jörg] [Borestein] [Peremans] [Ureña 1] [Polaroid] [Kleeman 2]. Usually, transducers work as emitters and as receivers in these systems, so the reception modules have to be disabled during the emission process to avoid interferences. In this way, echoes from near reflectors are discarded if they arrive during this emission interval. In Figure 9 a scheme about it is shown, where the value d_{min} means the minimum distance measured by a transducer. The value d_{min} is determined in (6).

$$d_{min} = \frac{c \cdot t_e}{2} \tag{6}$$

Where c is the propagation speed of ultrasounds (approximately 340 m/s); and t_e is the necessary time to carry out the ultrasonic emission.

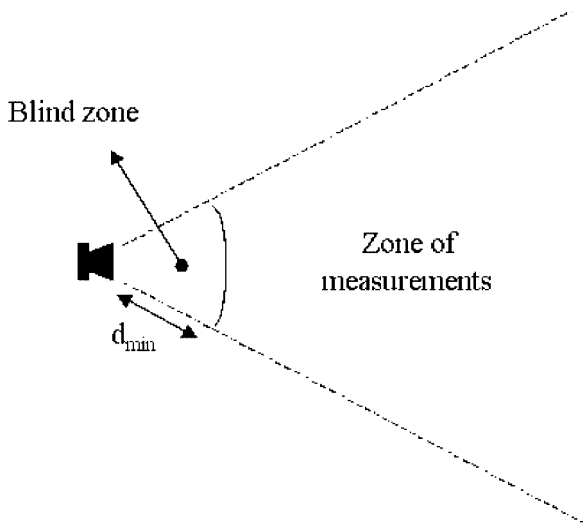


Figure 9. Scheme about the blind zone in an ultrasonic transducer.

Nevertheless, the use of Golay sequences has the additional advantage of overcoming this constraint. For an ideal auto-correlation of a Golay complementary sequence pair, the result of this computation is an ideal peak with an amplitude of $2 \cdot N \cdot M \cdot m$ (assuming the received signal $r_i[n]$ is normalized between -1 and $+1$). Where N is the length of the sequences, and M and m are the modulation parameters. The immediate consequence of having a reflector near to a transducer i is that, in the received signal $r_i[n]$, the reflected echo will be overlapped with the coupled emission during a determined interval. Figure 10 shows the corresponding power stage connected to the ultrasonic transducer, and based on a Polaroid 6500 series module [Polaroid]. According to it, during the emission phase, voltages around 300V are applied to the ultrasonic transducer in order to emit a determined signal.

As this coupled emission saturates the reception stage, there is a loss in the reflected echo. The advantage provided by Golay complementary sequences is that, even when a significant part of the signal is lost, the auto-correlation function provides a peak with enough amplitude to consider it as a valid echo (it should be taken into account that near reflectors provide echoes with better signal-to-noise ratios). Figure 11 shows the ideal result when a whole echo is processed: the maximum value achieves 512 units, corresponding to the parameters $N = 32$, $M = 8$ and $m = 2$. On the contrary, Figures 12 and 13 explain other different cases, where a part of the echo has been lost: 1/4 and 1/2 over the whole echo, respectively. It can be observed how the amplitude of the obtained peak decreases, but peaks can be still detected and considered as valid echoes.

In Figure 14 a timing example is shown to describe how echoes are detected when they are overlapped with the coupled emission. The emission interval t_e determines the period of emission coupling. This time t_e is determined by the sequence length N , by the modulation parameters m and M , and by the minimum separation among echoes L , according to (7).

$$t_e = T_s (m \cdot M \cdot N + L) \tag{7}$$

Where T_s is the sampling period, or time between two successive samples.

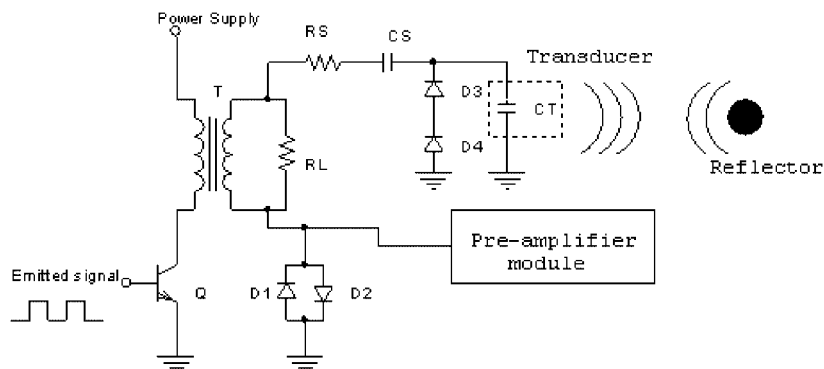


Figure 10. Electrical equivalent circuit of the used Polaroid 6500 series module [Polaroid].

If a reflector is near transducer i , an echo is received delayed with an interval t_i (see Figure 14), corresponding to the measured TOF. In this way, the system processes both receptions (one from the coupled emission, and another from a near echo), discriminating the local maximums from both with a delay of L , as it can be observed in Figure 14. Experimentally, it has been verified that reflectors can be detected correctly at distances up to 5 cm, assuming normal indoor environmental conditions, and using 32-bit Golay complementary sequences. This implies that the 78% over the whole echo is lost, overlapped by the coupled emission.

In Figure 15 and Figure 16 two examples of real scenarios are shown, in which a reflector has been placed on the axial axis of

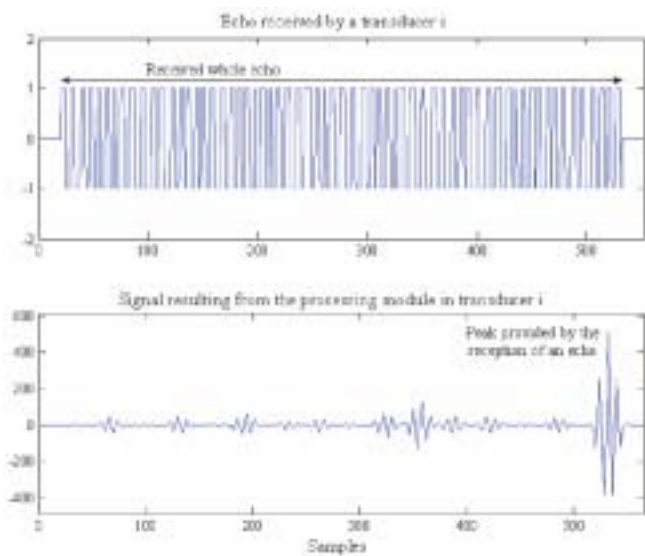


Figure 11. Ideal peak processed from the reception of a whole echo.

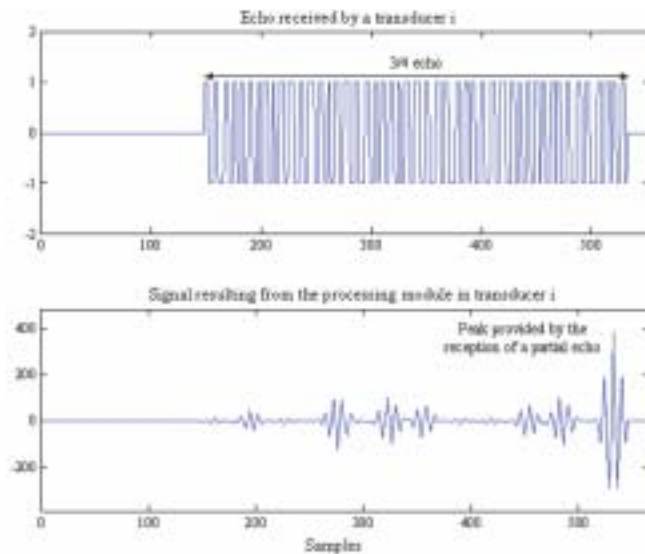


Figure 12. Resulting peak with a loss of 1/4 over the whole echo.

a transducer i . The top graph shows the signal $r_i[n]$ received by transducer i ; whereas, the processed signal $s_i[n]$ appears in the middle one, and finally, in the bottom graph, the result $p_i[n]$ from the peak detector is shown.

In the first example, the obstacle, a cylinder with a diameter $\phi = 3.5$ cm, is $d = 20$ cm far away (see Figure 7) on the axial axis of the transducer, whereas in the second one, it is $d = 10$ cm far away. Although, it can be observed in both how the emission and the reflected echo are overlapped in the acquired signal $r_i[n]$, the echoes corresponding to the reflectors placed inside the blind zone of the transducer are detected clearly (see the bottom graph of both figures). The second echo, called *Echo from reflector*, corresponds to the direct reflection from the obstacle. On the other hand, as a consequence of enabling the reception while the emission is performed, this one will be coupled causing a first maximum value, detected as a valid echo (see the

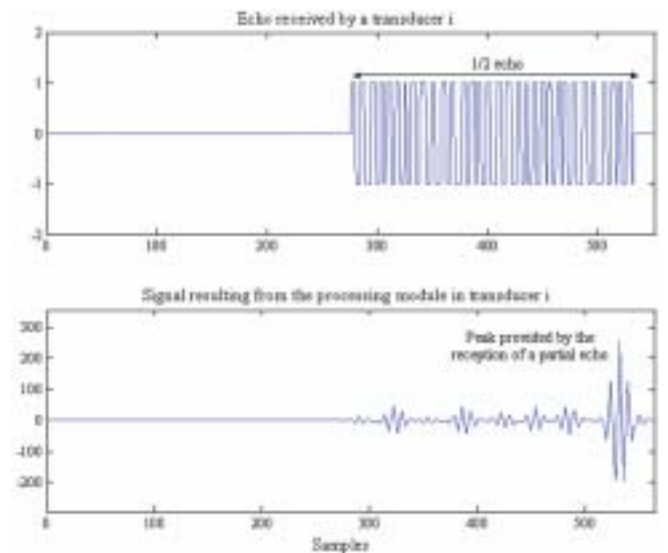


Figure 13. Resulting peak with a loss of 1/2 over the whole echo.

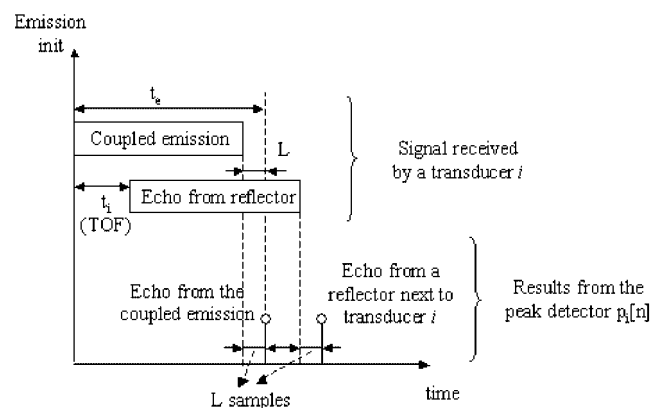


Figure 14. Timing of the reception of echoes from reflectors near transducers.

mentioned figures). However, the solution to this situation is immediate: those peaks, inside the emission interval t_e , should not be considered as valid echoes.

Notice the importance of this characteristic, which allows to reduce the blind area at a negligible distance, being possible to use transducers as emitters and as receivers in advanced sonar modules.

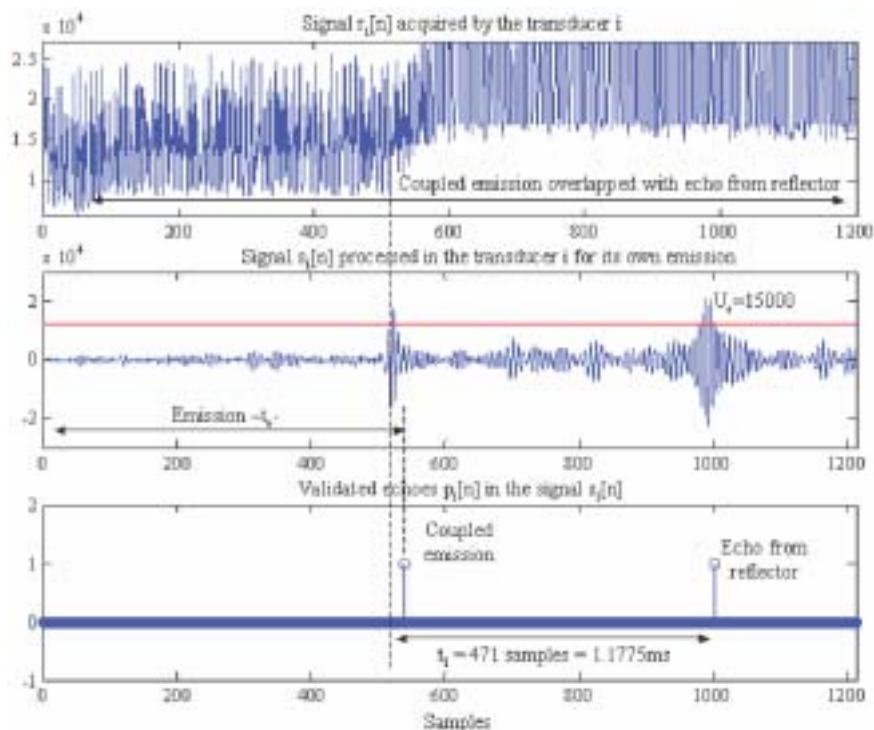


Figure 15. Results obtained for a reflector placed at 20 cm on the axial axis of the transducer i .

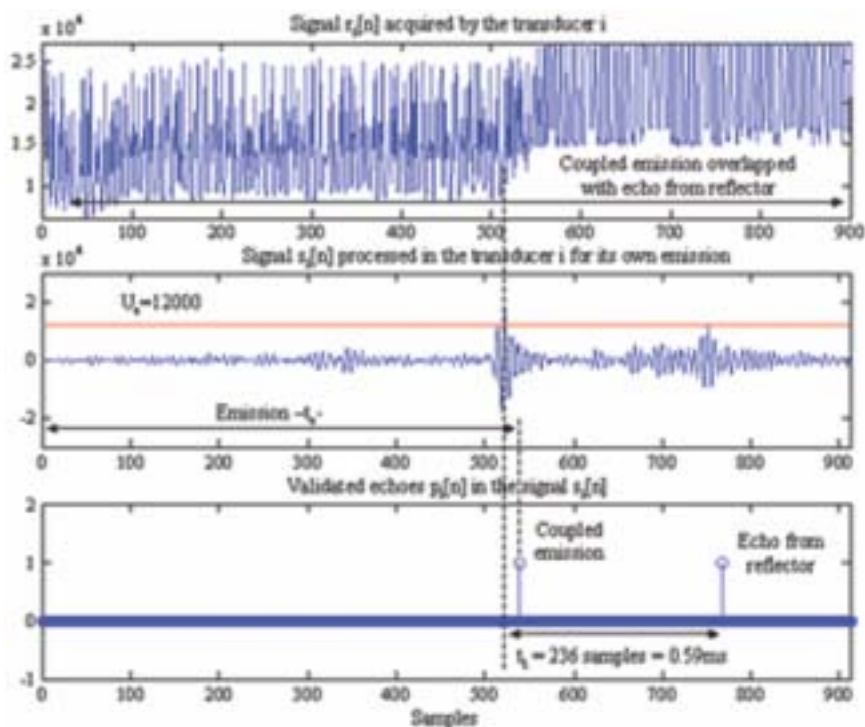


Figure 16. Results obtained for a reflector placed at 10 cm on the axial axis of the transducer i .

6. Conclusions

As tested in previous sections, the implemented algorithms allow sub-millimeter precisions to be obtained in the determination of distances among reflectors and transducers. This precision is basic, since it enables the later use of geometrical and trigonometric considerations in high-level processing. Otherwise, when measurements are not so precise, the high-level algorithms proposed for the construction of maps, or for the reflector classification, are less reliable. The precision achieved depends strongly on the length of the Golay sequences used. Several tests have been carried out with 32, 64 and 128 bits. For the case of 32 bits, a precision around 1mm is obtained at distances of 300 cm, and below 1mm for shorter distances. On the other hand, using 128 bits, precision is 0.5 mm at 300 cm and only 1.6mm at distances of 600 cm.

Furthermore, the use of Golay sequences allows to loose a part of the received echoes, due to the overlapping with the coupled emission. It is not so important if a percentage of the echo is overlapped and lost by the emission, since the intrinsic characteristics of Golay sequences allow the discrimination of the real echo. This feature is very interesting, keeping in mind that most sonar modules present the constraint of having a minimum distance below which it is not possible to detect a reflector. With the system here proposed, this constraint disappears, and echoes can be processed at shorter distances, even with long sequences. Experimentally, it has been determined that it is possible to detect obstacles placed up to distances of only 5 cm far away, what implies to reduce the blind zone to negligible figures.

The obtained results allow to use the processing system for ultrasonic transducers, in order to improve their performances. In this way, it is possible to associate several transducers in more complex sonar systems, as the one shown, where emission and reception can be carried out simultaneously by some transducers. This permits to reduce the scanning time and to obtain more information from the environment. Also, the achieved precision allows to develop high-level algorithms, as reflector classification or mapping, using TOFs determined by ultrasonic transducers.

References

- [Audenaert] K. AUDENAERT, H. PEREMANS, Y. KAWAHARA, J. VAN CAMPENHOUT, "Accurate ranging of multiple objects using ultrasonic sensors", *Proc. of IEEE Int. Conf. on Robotics and Automation*, 1992, p. 1733-1738.
- [Barshan] B. BARSHAN, B. AYRULU, "A comparison of four methods for accurate ultrasonic range estimation", *Proc. of 1st IEEE Balkan Conf. on Signal Processing, Communications, Circuits and Systems*, 2000.
- [Borestein] J. BORESTEIN, Y. KOREN, "Histogramic in-motion mapping for mobile robot obstacle avoidance", *IEEE Trans. on Robotics and Automation*, vol. 7, no. 4, 1991, p. 535-539.
- [Budisin] S.Z. BUDISIN, "Efficient pulse compressor for Golay complementary sequences", *Electronics Letters*, vol. 27, no. 3, 1991, p. 219-220.
- [Díaz] V. DÍAZ, J. UREÑA, M. MAZO, J.J. GARCÍA, E. BUENO, A. HERNÁNDEZ, "Using Golay complementary sequences for multi-mode ultrasonic operation", *Proc. of 1999 7th IEEE Int. Conf. on Emerging Technologies and Factory Automation (ETFA'99)*, Barcelona (Spain), 1999, p. 599-604.
- [O'Donovan] T.L. O'DONOVAN, P. ACEVEDO COSTA, D.K. DAS-GUPTA, "Application of Golay codes and piezoelectric ultrasound transducers to biomedical noninvasive measurement", *IEEE Trans. on Electrical Insulation*, vol. 28, no. 1, 1993, p. 93-100.
- [Elfes] A. ELFES, "Sonar based real-world mapping and navigation", *IEEE Journal of Robotics and Automation*, vol. RA-3, no. 3, 1987, p. 249-264.
- [Golay] M.J.E. GOLAY, "Complementary sequences", *IRE Trans. Information Theory*, IT-7, 1961, p. 82-87.
- [Hayward] G. HAYWARD, Y. GORFU, "A digital hardware correlation system for fast ultrasonic data acquisition in peak lower limited applications", *IEEE Trans. on Ultrasonic, Ferroelectrics, and Frequency Control*, vol. 35, no. 6, 1988, p. 800-808.
- [Hernández 1] A. HERNÁNDEZ, J. UREÑA, J.J. GARCÍA, M. MAZO, J.P. DÉRUTIN, J. SÉROT, "Ultrasonic sensor performance improvement using DSP-FPGA based architectures", *Proc. of 2002 28th IEEE Int. Conf. on Industrial Electronics, Control and Instrumentation (IECON'02)*, Sevilla (Spain), 2002, p. 2694-2699.
- [Hernández 2] A. HERNÁNDEZ, J. UREÑA, M. MAZO, J.J. GARCÍA, J.A. JIMÉNEZ, F.J. ÁLVAREZ, "Advanced sonar module for mapping applications", *Proc. of 9th IEEE Conference on Emerging Technologies and Factory Automation (ETFA'03)*, Lisboa (Portugal), 2003, p. 700-707.
- [Hovanessian] S.A. HOVANESSIAN, "Radar system design and analysis", Artech House Inc., Norwood, 1984.
- [Jörg] K. JÖRG, M. BERG, "First results in eliminating crosstalk & noise by applying pseudo-random sequences to mobile robot sonar sensing", *Proc. of IEEE/RJSJ Int. Conf. on Intelligent Robots and Systems (IROS'96)*, Osaka (Japan), 1996.
- [Kim] B.H. KIM, T.H. KIM, T.K. SONG, "Generation of mutually orthogonal polyphase complementary sequences for use in ultrasound imaging", *Proc. of 2002 IEEE Ultrasonics Symposium*, 2002, p. 1693-1696.
- [Kleeman 1] L. KLEEMAN, R. KUC, "Mobile robot sonar for target localization and classification", *The International Journal of Robotics Research*, vol. 14, no. 4, 1995, p. 295-318.
- [Kleeman 2] L. KLEEMAN, "Advanced sonar sensing", *Proc. of 10th International Symposium on Robotics Research (ISRR'01)*, Lorne (Australia), 2001, p. 286-295.
- [Lee] B.B. LEE, E.S. FURGASON, "High speed digital Golay code flaw detection system", *IEEE Ultrasonics Symposium*, vol. 21, no.4, 1983, p. 153-161.
- [Papageorgiou] C. PAPAGEORGIOU, C. KOSMATOPOULOS, T. LAOPOULOS, "Accurate time-of-flight measurement of ultrasonic signals for displacement monitoring applications", *Proc. of IEEE Instrumentation and Measurement Technology Conf.*, St. Paul (USA), 1998, p. 154-159.
- [Peremans] H. PEREMANS, K. AUDENAERT, J.M. VAN CAMPENHOUT, "A high resolution sensor based on tri-aural perception", *IEEE Trans. on Robotics and Automation*, vol. 9, no. 1, 1993, p. 36-48.
- [Polaroid] POLAROID CORPORATION, "Ultrasonic ranging systems", 1991.
- [Popovic] B.M. POPOVIC, "Efficient Golay correlator", *IEE Electronics Letters*, vol. 35, no. 17, 1999, p. 1427-1428.
- [Sabatini] A.M. SABATINI, "Active hearing for external imaging based on an ultrasonic transducer array", *Proc. of IEEE Int. Conf. on Intelligent Robots and Systems (IROS'92)*, Raleigh (USA), 1992, p. 829-836.
- [Shoval] S. SHOVAL, J. BORESTEIN, "Using coded signals to benefit from ultrasonic sensor crosstalk in mobile robots obstacle avoidance", *Proc. of 2001 IEEE Int. Conf. on Robotics and Automation (ICRA'01)*, Seoul (Korea), 2001, p. 2879-2884.

[Tseng] C.C. TSENG, C.L. LIU, "Complementary sets of sequences", *IEEE Trans. on Information Theory*, vol. IT-18, no. 5, 1972, p. 644-652.

[Ureña 1] J. UREÑA, M. MAZO, J.J. GARCÍA, A. HERNÁNDEZ, E. BUENO, "Correlation detector based on a FPGA for ultrasonic sensors", *Microprocessors and Microsystems*, no. 23, 1999, p. 25-33.

[Ureña 2] J. UREÑA, M. MAZO, J.J. GARCÍA, A. HERNÁNDEZ, E. BUENO, "Classification of reflectors with an ultrasonic sensor for mobile robot applications", *Robotics and Autonomous Systems*, vol. 29, 1999, p. 229-279.

[Yoo] Y.M. YOO, W.Y. LEE, T.K. SONG, "A low voltage portable system using modified Golay sequences", *Proc. of 2001 IEEE Ultrasonics Symposium*, 2001, p. 1469-1472.



Álvaro Hernández

Álvaro Hernández obtained his Electronic Engineering degree from the University of Alcalá (Spain) in 1998. In 2003, he obtained his PhD from the University of Alcalá (Spain), and from the Blaise Pascal University (France). He is currently an Associate Professor of Digital Systems at the Electronics Department in the University of Alcalá. His research areas are multi-sensor integration, electronic systems for mobile robots, digital systems and computing architectures.



Jesús Ureña

Jesús Ureña received the Telecommunications Engineering (MS) from the Polytechnical University of Madrid (Spain) in 1992; and his Ph.D. degree in Telecommunications from the University of Alcalá (Spain) in 1998. Since 1986 he has been a lecturer of the Electronics Department at the University of Alcalá. His current research areas are low-level ultrasonic signal processing, local positioning systems (LPS) and sensory systems for railway safety.



Manuel Mazo

Manuel Mazo received his PhD degree in telecommunications in 1988, and his engineering degree (M.Sc) in telecommunications in 1982, all of them from the Polytechnic University of Madrid (Spain). Currently, he is a professor of the Electronics Department at the University of Alcalá. His research areas are multi-sensor (ultrasonic, infrared and artificial vision) integration and electronic control systems applied to for railway safety, mobile robots and wheelchairs for physically disabled people.



José A. Jiménez

José A. Jiménez obtained his Electronic Telecommunication Engineering degree in 1996 from the University of Valencia (Spain). In 2004, he obtained his PhD from the University of Alcalá (Spain). He is currently an Associate Professor of Instrumentation Electronics in the Electronics Department at the University of Alcalá. His research areas are sensorial systems applied to robotic, instrumentation and electronic systems for mobile robots.



Fernando Álvarez

Fernando Álvarez obtained his Physics degree from the University of Sevilla (Spain) in 1998. He is currently an Assistant Professor of Control Engineering at the Electronics Department in the University of Extremadura (Spain). His research areas are low-level ultrasonic signal processing and sensory systems for railway safety.



Juan Jesús García

Juan Jesús García obtained his Telecommunication Engineering degree in 1998 from the University of Valencia (Spain). He has been a Associate Professor of Analog and Digital Electronics in the Electronics Department in the University of Alcalá since 1994. He has worked on several public and private projects related to Digital Control and Sensors Systems, and his current areas of interest are Mobile Robots and Multi-sensor Integration.



Jean-Pierre **Dérutin**

Jean-Pierre Dérutin has been a Professor at the Blaise Pascal University in Clermont-Ferrand (France) from 1994. He received his HDR degree in 1993 at the same university. He is Co-director of GRAVIR group at LASMEA- UMR 6602 CNRS- and responsible for the "Architectures et programmation des machines de perception" Group. His research areas are MIMD-DM models for vision machines, their programming, and prototype methodologies for applications on these architectures. Also, he works with configurable architectures, using FPGA or SOPC devices.



Jocelyn **Sérot**

Jocelyn Sérot graduated from IRESTE, Nantes in 1989 and received the PhD degree from the University of Paris-Sud in 1993. He is now Associate Professor at the Blaise Pascal University, Clermont-Ferrand, France. He works within the Computer Vision group of LASMEA (Laboratoire des Sciences et Matériaux pour l'Electronique, et d'Automatique) CNRS laboratory.



